JOURNAL OF OPTOELECTRONICS AND ADVANCED MATERIALS Vol. 8, No. 5, October 2006, p. 1685 - 1690

Invited Paper

Preparation and characterization of Fe-(Cr,Mo,Ga)-(P,C,B) soft magnetic bulk metallic glasses

M. STOICA[a,b*], J. ECKERT[c], S. ROTH[a], L. SCHULTZ[a], A. R. YAVARI[b]
[a]*IFW Dresden, Institute for Metallic Materials, P.O. Box 270016, D-01171 Dresden, Germany*
[b]*LTPCM-CNRS UA29, ENSEEG, Institut National Politechnique de Grenoble, Domain Universitaire, 1130 Rue de la Piscine, BP 75 Saint Martin d'Hères Campus 38402, France*
[c]*TU Darmstadt, Department of Materials and Earth Sciences, Physical Metallurgy Division, Petersenstrasse 23, D-64287 Darmstadt, Germany*

Using master alloys with nominal compositions $Fe_{77.5-x-y-z}Cr_xMo_yGa_zP_{12}C_5B_{5.5}$ (x,y,z = 4,4,4; 4,4,2; 4,4,0 and 2,2,2), cylindrical rods up to 3 mm in diameter and 70 mm in length, rectangular bars 2 × 2 mm and 30 mm length and discs with 10 mm in diameter and 1 mm thickness were produced using the copper mold casting technique. By powder metallurgical methods, pellets with even larger dimensions (10 mm in diameter and 3-5 mm in thickness) were prepared. Compression tests reveal that the fracture strength for the as-cast samples σ_f is around 3 GPa and the fracture strain ε_f reaches 2 %. Upon annealing, the fracture strain drops to 1.6 % and no plastic deformation is observed while the fracture stress remains almost the same. The coercivity of the as-cast samples is lower than 10 A/m, decreasing to 0.7 A/m upon annealing. The coercivity of as-milled powder is greater than 1000 A/m, and it decreases to 25 A/m after hot compaction and subsequent annealing, although the latter value is one order of magnitude higher than those for cast samples.

(Received September 5, 2006; accepted September 13, 2006)

Keywords: Bulk metallic glasses, Magnetic properties, Mechanical characterization

1. Introduction

Amorphous alloys are good candidates for application as soft magnetic materials because of the lack of crystal anisotropy. The only sources of undemanded anisotropies are the shape anisotropy due to surface roughness and the stress-induced anisotropy caused by the stress resulting from rapid quenching [1,2]. This is why amorphous soft magnetic materials became an established class of materials. Amorphous materials with enhanced glass formability give an opportunity to improve the value in use of amorphous materials further. It may be possible to cast such alloys directly for use as components of magnetic cores. Although conventional soft magnetic alloys have higher saturation magnetization compared to the amorphous alloys, the latter often have very high mechanical strength and high resistance against corrosion which may be important for application as magnetic parts in valves, clutches, or relays.

The critical cooling rate of about 100 K/s necessary for glass formation is higher than the value of about 1-10 K/s characteristic for non-magnetic alloys with very good glass-forming ability [3,4]. Thus, the maximum diameter of these Fe-based alloys is limited to only a few millimeters [5], in contrast to Zr- or Cu-based glassy alloys, which can easily reach even 10 mm diameter [6]. Only very recently, Ponnambalam *et al*. [7] and, independently, Lu *et al.* [8] succeeded to cast Fe-based BMGs with a thickness larger than one centimeter (using some small addition of Y, Ln and/or Er), but their glasses are paramagnetic at room temperature, with a Curie temperature of around 55 K. The difficulty to cast such ferrous glasses in bulk form is one of the reasons for why, despite an increasing number of published papers about the mechanical properties of BMGs, most of these reports deal only with non-ferrous Zr-, Ti- or Cu- based [6,9,10].

The "birth year" of the Fe-(Cr,Mo,Ga)-(P,C,B) alloys used for investigations in this work can be considered 1999, when T.D. Shen and R.B. Schwarz from Los Alamos National Laboratory USA (LANL) published the paper entitled "Bulk ferromagnetic glasses prepared by flux melting and water quenching" in *Applied Physics Letters* [11]. They cast such alloys in rod shape with a maximum diameter of 4 mm. Using similar compositions, in our lab cylindrical rods up to 3 mm diameter and 70 mm length, rectangular bars 2 × 2 mm and 30 mm length and discs with 10 mm diameter and 1 mm thickness were produced using the copper mold casting technique.

On the other hand, bulk amorphous samples with various sizes and shapes can be prepared by mechanical alloying or ball milling of amorphous ribbons combined with subsequent consolidation of the resulting powders in the viscous state at temperatures in the supercooled liquid region [12,13], which is defined as the difference between crystallization temperature T_x and glass transition temperature T_g. High-energy ball milling induces stresses, which can be successfully reduced by annealing the resulting powders at temperatures below the onset of crystallization [14,15]. The enhanced coercivity of ball milled powders in comparison with melt-spun ribbons is due not only by the mechanical stress induced upon milling, but it may be caused also by presence of nonmagnetic oxide phases formed during milling on the reactive surface of the powder particles [14]. The

consolidation process can be combined with annealing in order to obtain bulk specimens with amorphous structure. This can yield bulk amorphous specimens with larger dimensions than those achievable by slow cooling from the melt [16]. By such powder metallurgical methods were prepared pellets with 10 mm in diameter and 3-5 mm in thickness, i.e. larger dimensions than those obtained in the case of copper mold casting. Consequently, this work focuses on the possibility to prepare such bulk metallic glasses using copper mold casting technique and powder metallurgical methods, as well as to their mechanical and magnetic properties.

2. Experimental

Several $Fe_{77.5-x-y-z}Cr_xMo_yGa_zP_{12}C_5B_{5.5}$ master alloys with different Fe, Cr, Mo and Ga content were produced using induction melting. The preparation consisted of several steps. The first step was dedicated to produce binary FeC, FeGa and FeP pre-alloys. Subsequently they were melted together with pure Cr, Mo and B in the necessary proportions. The raw materials used in present study were: bulk pieces of Fe, Ga, Cr and Mo with a purity better than 99.9%, graphite as C– powder with 99.9% purity, crystalline B with 99.999% purity and red amorphous P– powder with 99% purity. The FeP pre-alloy was prepared by mechanical alloying of Fe powder (less than 10 microns particle size) with P powder (less than 100 microns particle size) in a SPEX 8000 shaker mill, consolidation of the alloyed powder by cold pressing and subsequent induction melting of the resulting pellets. The handling of the powder was done in a glove box, under purified Ar atmosphere with less than 1 ppm oxygen and water content. The FeC pre-alloy was obtained by induction melting of Fe lumps together with graphite powder. Fe lumps melted together with Ga lumps gave the third pre-alloy, with the composition $Fe_{56.36}Ga_{43.64}$.

The amorphous ribbons were prepared by single-roller melt spinning on a copper wheel under argon flow at 24 $m \cdot s^{-1}$ tangential velocity of the wheel. Some parts of these ribbons were cut into small pieces, ball-milled and subsequently compacted to discs of 10 mm in diameter and 3-5 mm in thickness. The milling experiments were done in a Retsch PM 4000 planetary ball mill under an argon atmosphere using hardened steel balls and vials and the ball-to-powder weight ratio was 15:1. The sample handling was performed as described previously for FeP powders- in a glove box under purified argon atmosphere (< 1 ppm O_2 and H_2O). The consolidation of the resulting powders into bulk samples was done in an unaxial hot press under a vacuum of 10^{-3} Pa. The powder was heated at 0.67 $K \cdot s^{-1}$ to the consolidation temperature, held isothermally at this temperature and compacted at a pressure of 500 MPa. The sample was held isothermally in the press under the applied load for 2 min. The compacting temperatures were chosen to be in the temperature range of the supercooled liquid region.

A PHILIPS PW 3020 Bragg-Brentano diffractometer using CoK_α (λ = 1.78897 Å) radiation was used in order to identify the phases formed upon fast cooling or upon milling and subsequent hot pressing of the resulted powders. The samples were prepared by crushing the glassy alloys into small pieces and bonded into amorphous resin in order to have a good resolution. The same type of preparation was applied for powder samples.

The room temperature stress (σ) versus strain (ε) curves under compression were measured using an INSTRON 8562 device, for cylindrical and rectangular samples, in the as-cast as well as in the annealed state. The samples were cut in small pieces, with the length being equal to twice the diameter in the case of cylinders or twice the diagonal, in the case of bars. The faces perpendicular to the longitudinal axis were carefully polished and checked to be parallel. The hardness of the amorphous alloys was measured using a computer-controlled Struers Duramin 5 Vickers hardness tester. The applied load was 1.96 N for 10 seconds. The final result is an average of more than 15 measured data.

For measuring the coercivity of the very soft magnetic alloys, a DC Förster Coercimat working at 200 kA/m magnetizing field was used. The polarization at saturation was measured with a vibrating sample magnetometer under magnetic DC fields up to 20 kOe ($\mu_0 H$ = 2 T).

3. Results and discussion

Figs. 1 (a), (b), (c) and (d) show typical diffraction patterns for various samples and compositions. Generally, the patterns only consist of a broad diffraction maximum centred at 2θ = 51°, which is characteristic for an amorphous phase. However, it is rather difficult to rule out the existence of a small volume fraction of nanoscale crystalline precipitates, which may be present in the glassy matrix. For example, there are additional diffraction peaks with weak intensity superimposed on the broad diffraction maximum of the amorphous phase for the $Fe_{65.5}Cr_4Mo_4Ga_4P_{12}C_5B_{5.5}$ cast rod with 3 mm diameter (Fig. 1 (a)). The 1.5 mm diameter $Fe_{67.5}Cr_4Mo_4Ga_2P_{12}C_5B_{5.5}$ rod exhibits the same behavior (see Fig. 1 (b)). In the case of $Fe_{69.5}Cr_4Mo_4P_{12}C_5B_{5.5}$, the composition without Ga, the number of such nanocrystalline inclusions is high enough to produce clear crystalline reflections for the rod with 1.5 mm diameter (Fig. 1 (c)). The maximum achievable diameter for which the samples are still fully amorphous decreases with decreasing Ga content, i.e. the glass-forming ability deteriorates with decreasing Ga content. In the case of $Fe_{71.5}Cr_2Mo_2Ga_2P_{12}C_5B_{5.5}$, it was not possible to cast an amorphous rod using the copper mold casting method, even for small diameters. Figure 1 (d) shows the diffraction pattern of a $Fe_{71.5}Cr_2Mo_2Ga_2P_{12}C_5B_{5.5}$ melt-spun ribbon.

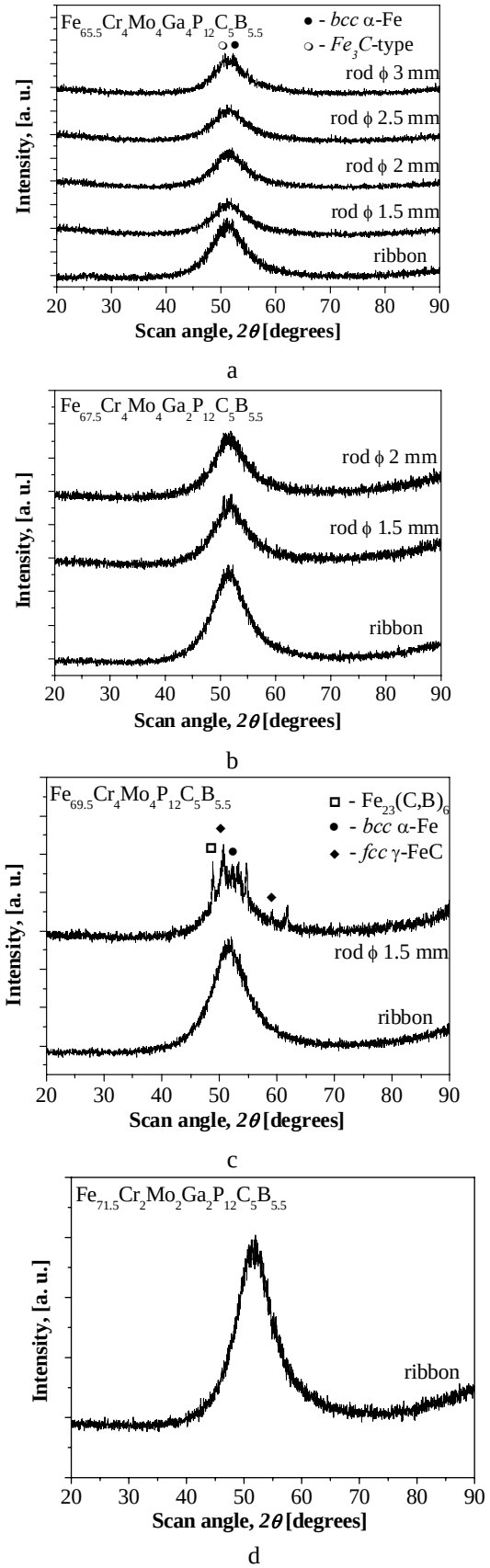

Fig. 1. X-ray diffraction patterns for different samples and compositions: (a) $Fe_{65.5}Cr_4Mo_4Ga_4P_{12}C_5B_{5.5}$, (b) $Fe_{67.5}Cr_4Mo_4Ga_2P_{12}C_5B_{5.5}$, (c) $Fe_{69.5}Cr_4Mo_4P_{12}C_5B_{5.5}$ and (d) $Fe_{71.5}Cr_2Mo_2Ga_2P_{12}C_5B_{5.5}$.

The wave vector Q, related to the wavelength λ and to the scan angle θ by $Q = (4\pi \sin\theta)/\lambda$ [18], can be calculated. The position of the main broad diffraction peak slightly changes with varying composition: Q = 30.51 nm^{-1} for $Fe_{65.5}Cr_4Mo_4Ga_4P_{12}C_5B_{5.5}$, 30.68 nm^{-1} for $Fe_{67.5}Cr_4Mo_4Ga_2P_{12}C_5B_{5.5}$, 30.75 nm^{-1} for $Fe_{69.5}Cr_4Mo_4P_{12}C_5B_{5.5}$. For the melt-spun ribbon with the composition $Fe_{71.5}Cr_2Mo_2Ga_2P_{12}C_5B_{5.5}$, which was fully amorphous, Q = 30.71 nm^{-1} (Fig. 1 (d)). The angular positions of the amorphous peaks depend on the short-range atomic order of the samples. A better atomic compaction shifts the wave vector Q towards higher values [19]. The trend observed for the first three compositions, i.e. the increase of the wave vector Q with increasing Fe content, can be attributed to an atomic structure which becomes more packed when the number of Ga atoms decreases and the number of Fe atoms increases. This is easy to anticipate, because the atomic radius of Fe is smaller than the atomic radius of Ga [20] and the atoms can arrange in a more compact structure.

Bulk amorphous samples with larger geometrical dimensions can be obtained using the powder metallurgical technique. For that, the amorphous melt-spun ribbons were cut in small pieces, ball-milled and hot compacted. For these experiments, the $Fe_{65.5}Cr_4Mo_4Ga_4P_{12}C_5B_{5.5}$ composition was chosen, because it exhibits the best glass-forming ability among the studied compositions. The rotational velocity of the planetary ball mill can be considered as a rough estimate of the milling intensity. In order to study the influence of milling conditions, three different velocities were used, while keeping the milling time constant (3 hours). The initial ribbons, named R1, R2 and R3, were identically from the structural point of view (completely amorphous – see Fig. 2 (a)). The X-ray diffraction experiments performed for the powders (P1, P2 and P3 denote the powders of ribbons R1, R2 and R3, which were milled at 200, 250 and 300 RPM, respectively), revealed also a fully amorphous structure (Fig. 2 (b)).

The broad maxima, characteristic for an amorphous phase, are centred at 2θ = 51.5° (Q = 30.51 nm^{-1}) in the case of melt-spun ribbons. Upon milling, the maxima are shifted towards higher values: Q = 30.58 nm^{-1} for powder P1, 30.59 nm^{-1} for powder P2 and 30.62 nm^{-1} for powder P3. As was recently published [19,21], the higher values of Q can be attributed to an increase free volume content. The amount of free volume, which is generated upon milling, is proportional to the milling intensity: the higher the velocity, the more the excess free volume. This agrees well with a free-volume generation during heterogeneous plastic deformation of metallic glasses [22].

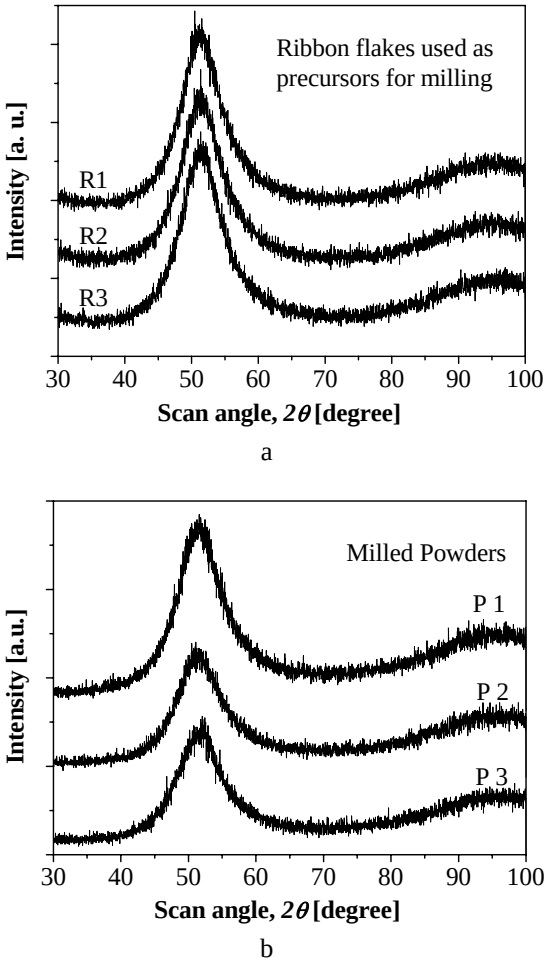

Fig. 2. XRD patterns corresponding to amorphous $Fe_{65.5}Cr_4Mo_4Ga_4P_{12}C_5B_{5.5}$ ribbons before milling (a) and to resulted powders after milling (P1 at 200 RPM, P2 at 250 RPM and P3 at 300 RPM) (b).

Fig. 3 (a) shows the compressive stress-strain curves for the as-cast $Fe_{65.5}Cr_4Mo_4Ga_4P_{12}C_5B_{5.5}$ cylindrical rods with 2 and 2.5 mm diameter, respectively. Both samples exhibit similar features, i.e. an elastic deformation regime followed by a small compressive plastic strain. The yield stress σ_y, measured at the offset yield, is 3.19 GPa for the 2 mm diameter sample and 3.27 GPa for the 2.5 mm diameter sample. The corresponding elastic strain ε_y is 2.03 % for the 2 mm diameter rod and 1.91 % for the 2.5 mm diameter rod, respectively. Young's modulus is determined as 160 GPa for the 2 mm diameter sample and 170 GPa for the 2.5 mm diameter sample. The fracture of the samples occurs at a fracture stress σ_f of 3.23 GPa for the 2 mm diameter sample. σ_f reaches 3.27 GPa for the 2.5 mm diameter sample. The fracture strain ε_f is 2.33 % and 2.03 %, respectively. The pure compressive plastic strain is 0.30 % and 0.12 % for the two samples, respectively. Hence, this Fe-based bulk glass exhibits a very high strength, higher than that observed in the case of non-ferrous bulk amorphous alloys (1.5 – 1.8 GPa for Zr-based alloys, 1.7 – 1.9 GPa for Ti-based alloys or 1.9 – 2.5 GPa for Cu-based alloys [6,10,23]), but close to that measured for Fe-B-Si-Nb (3.25 GPa) and Fe-Ga-P-C-B-Si systems (3.16 GPa) [24]. The compressive behavior of the rod with 2.5 mm diameter is slightly different in comparison to the rod with 2 mm diameter (see Fig. 3 (a)). The differences between the two described samples regarding their mechanical data are quite small and are within the limits of error of the measurement. The error in the measurement of the small cross-section of the sample is 5 % and is comparable with the difference between the two calculated values for Young's modulus (160 GPa for the 2 mm and 170 GPa for the 2.5 mm diameter sample, respectively).

Fig. 3 (b) shows the compressive stress-strain curves for as-cast and annealed rectangular bars with the cross section 2 mm × 2 mm. The yield stress is 2.82 GPa and 2.84 GPa for the as-cast and for the annealed sample, respectively. The corresponding compressive elastic strains are 1.76 % and 1.60 %, respectively. Young's modulus is 161 GPa for the as-cast state and 177 GPa after annealing. The fracture of both samples occurs at nearly the same value of compressive stress, 2.84 GPa, but the corresponding fracture strain is different: 1.91 % for the as-cast sample and 1.63 % for the annealed one. The as-cast sample shows a small plastic deformation of 0.15 %, but in the case of the annealed bar the plastic regime extends only over 0.03 %.

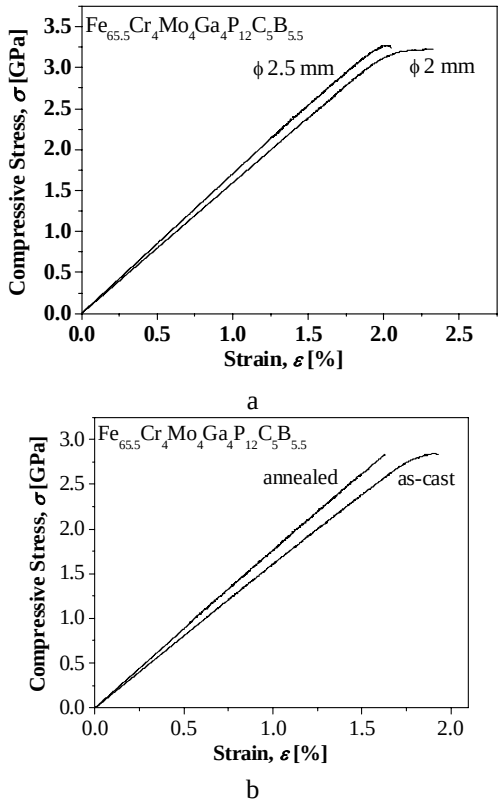

Fig. 3. Compressive stress-strain curves for: (a) as-cast $Fe_{65.5}Cr_4Mo_4Ga_4P_{12}C_5B_{5.5}$ 2 mm and 2.5 mm diameter rods and (b) $Fe_{65.5}Cr_4Mo_4Ga_4P_{12}C_5B_{5.5}$ as-cast and annealed rectangular bars. The samples were annealed for 10 min at 712 K, i.e., at a temperature equal to T_g – 15 K, using a heating and cooling rate of 5 K/min. It can be noted that the fracture stress retains almost the same value after annealing, but the sample becomes more brittle and no plastic deformation is observed.

The average value of the Vickers hardness for the as-cast bars is *HV* = 885 (8.68 GPa) with a typical standard deviation of 5. The hardness of the annealed bars increases up to *HV* = 902 (8.84 GPa) with a standard deviation of 2.1. The smaller value of the standard deviation in the case of the annealed samples indicates a more homogeneous behavior of the annealed specimens in comparison with the as-cast state. Upon annealing the hardness increases, because the annealing induces a structural relaxation and consequently density and packing slightly increase [25]. The mechanical properties follow the same trend, i.e. Young's modulus increases, the plasticity may drop and the hardness increases (Fig. 3 (b)).

The variation of the coercivity for fully amorphous samples as a function of annealing temperature is shown in Fig. 4. The annealing was performed in the DSC under a purified Ar flow and constant 5 K/min heating and cooling rate. One amorphous $Fe_{65.5}Cr_4Mo_4Ga_4P_{12}C_5B_{5.5}$ cast disc was cut in small slices and each piece was kept for 10 min at different annealing temperatures: 623 K, 723 K, 748 K, 753 K, 758 K, 763 K, 768 K, 773 K and 873 K, respectively. The glass transition temperature for this set of samples was found to be T_g = 727 K and the crystallization temperature T_x = 783 K (measured at 5 K/min heating rate). The hysteresis curves were modified also by such a kind of thermal treatments. For comparison, Fig. 5 shows the hysteresis loops recorded with the VSM, taken for slices from an $Fe_{65.5}Cr_4Mo_4Ga_4P_{12}C_5B_{5.5}$ glassy disc annealed for 10 min at 623 K and 723 K, respectively. The saturation magnetization increases upon annealing (from 78 Am^2/Kg to 85 Am^2/Kg), but by no more than 10 %. An important effect can be observed for the shape of the loops: the tendency is to become more rectangular and the approach to saturation is more rapid.

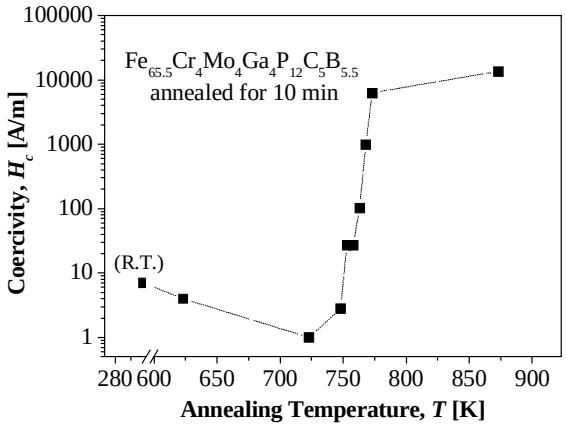

Fig. 4. Variation of the coercivity as a function of annealing temperature (R.T. = room temperature).

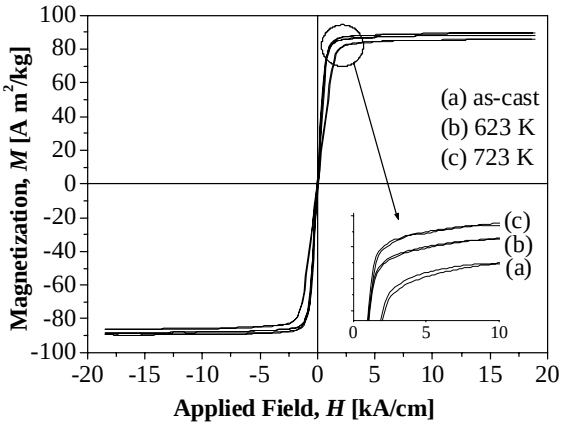

Fig. 5. Hysteresis loops of $Fe_{65.5}Cr_4Mo_4Ga_4P_{12}C_5B_{5.5}$ glassy samples as cast and after annealing.

Table 1 summarize the coercivity of as-milled ribbons, as-compacted compacted pellets, the pellets after a subsequent annealing as well as for the ribbon used as precursor. After hot compaction, the samples show a lower coercivity, but up to more than 100 times larger than the value of the as-quenched ribbon. A subsequent annealing can decrease these values. The final values are lower, but still at least one order of magnitude higher than those obtained for bulk cast samples.

Table 1. Coercivity of powder $Fe_{65.5}Cr_4Mo_4Ga_4P_{12}C_5B_{5.5}$ samples and ribbon used as precursor, together with the estimated values of relative density.

Sample	P1	P2	P3	Ribbon
Hc [A/m] as-milled	1090	1260	1500	–
Hc [A/m] as-compacted	50	60	190	1.7
Hc [A/m] annealed	23	37	135	< 1
Relative density of compacted pellets	80.58 %	79.40 %	76.83 %	100 %

The explanation for this behavior is related to the lower relative density, which characterizes the compacted samples, in contrast to the fully dense samples obtained upon copper mold casting. The presence of pores is magnetically the same as the presence of a second nonmagnetic phase and gives rise to a stray field. Thus magnetization reversal is bumped by the pores. The samples P1 and P2, with relatively close density values (80.58 % for P1 and 79.40 % for P2), exhibit also similar values of coercivity (23 A/m for P1 and 37 A/m for P2), but with a further decrease of the density (76.83 % for P3), the coercivity increases drastically: 135 A/m even after annealing. Another fact, which may help to explain this behavior, is the increase of the oxygen content with increasing milling velocity [14], where oxides are another non magnetic phase and may also act as sources of stress due to different thermal expansion.

4. Conclusions

The bulk amorphous $Fe_{65.5}Cr_4Mo_4Ga_4P_{12}C_5B_{5.5}$ samples with various shapes can be produced by copper mold as well as powder metallurgy. A high strength and some compressive plastic strain were observed upon compression test performed at room temperature. A structural relaxation treatment at elevated temperature does not affect the stress level, which remains almost the same, but the plasticity disappears. The magnetic behavior of amorphous samples prepared by both methods is characteristic for soft magnetic materials. The annealing, which reduces the plasticity of the samples, has a positive influence concerning the magnetic properties.

Aknowledgements

Financial support from the German Science Foundation under grant number EC 111/12-1 and from the EU within the framework of the RTN-networks on bulk metallic glasses (HPRN-CT-2000-00033) and ductile BMG composites (MRTN-CT-2003-504692) is acknowledged.

References

[1] A. Inoue, J. S. Gook, Mater. Trans. JIM **36,** 1180 (1995).
[2] H. S. Chen, Rep. Prog. Phys. **43**, 353 (1980).
[3] A. Inoue, A. Kato, T. Zhang, S. G. Kim, T. Masumoto, Mater. Trans. JIM **32,** 609 (1991).
[4] Y. He, T. Shen, R. B. Schwarz, Metall. Mater. Trans. A **29**, 1795 (1998).
[5] A. Inoue, T. Zhang, A. Takeuchi, Appl. Phys. Lett. **71,** 464 (1997).
[6] A. Inoue, Acta Mater. **48**, 279 (2000).
[7] V. Ponnambalam, S. J. Poon, G. J. Shiflet, J. Mater. Res. **19**, 1320 (2004).
[8] Z. P. Lu, C. T. Liu, J. R. Thomson, W. D. Porter, Phys. Rev. Lett. **92**, 245503 (2004).
[9] A. Inoue, Bulk Amorphous Alloys, Trans Tech Publications, Uetikon-Zuerich Switzerland, 1999.
[10] A. Inoue, W. Zhang, T. Zhang, K. Kurosaka, Acta Mater. **49**, 2645 (2001).
[11] T. D. Shen, R. B. Schwarz, Appl. Phys. Lett. **75**, 49 (1999).
[12] J. Eckert, N. Schlorke, C. A. R. T. Miranda, L. Schultz, Synthesis and Processing of Light Weight Mettalic Materials II, ed. C. M. Ward-Close et al., Warrendale: The Minerals Metals and Materials Society, 1997, p 383.
[13] M. Seidel, J. Eckert, H-D. Bauer, L. Schultz, Mater. Sci. Forum **119**, 225 (1996).
[14] N. Schlorke, J. Eckert, L. Schultz: J. Phys. D: Appl Phys. **32 ,** 855 (1999).
[15] N. Schlorke-de Boer, R. Schäfer, J. Eckert, L. Schultz, J. Appl. Phys. **91**, 6601 (2002).
[16] N. Schlorke-de Boer: Metallische Massivgläser auf Fe-Al-P-C-B-(Ga-) Basis und Verbund-materialien mit Mg-Y-Cu-Glas Matrix, Ph.D. Thesis, Technical University Dresden 2001.
[17] A. Gebert, J. Eckert, L. Schultz, Acta Mater. **46**, 5475 (1998).
[18] C. Kittel, Introduction to solid state physics, John Wiley & Sons Inc., New York (1953).
[19] A. R. Yavari, M. Tonegaru, N. Lupu, A. Inoue, E. Matsubara, G. Vaughan, Å. Kvick, Mat. Res. Soc. Symp. Proc. **806**, 203 (2004).
[20] ASM Handbook, vol. 1, 2 Metals Handbook, vol. 3 Alloy phase diagram, ASM International, Materials Park Ohio, USA (1992).
[21] K. Hajlaoui, T. Benameur, G. Vaughan, A. R. Yavari, Scripta Mater. **51**, 843 (2004).
[22] M. Heggen, F. Spaepen, M. Feuerbacher, Mat. Res. Soc. Symp. Proc. **806**, 307 (2004).
[23] C. Ma, A. Inoue, Mater. Trans. **44**, 188 (2003).
[24] A. Inoue, B. L. Shen, A. R. Yavari, A. L. Greer, J. Mater. Res. **18**, 1487 (2003).
[25] H. S. Chen, Rep. Prog. Phys. **43**, 353 (1980).

*Corresponding author: m.stoica@phm.tu-darmstadt